# Optimizing Bus Coupler Configuration of a Subsystem in Network Configuration considering Operational Constraints

Robbyo Ardiles Pakpahan[1]*, Lesnanto MultaPutranto[1], Fransisco Danang Wijaya[1]

[1] Department of Electrical & Information Engineering, Universitas Gadjah Mada, Yogyakarta, Indonesia
robbyoardilespakpahan@mail.ugm.ac.id

**Abstract.** The Java, Madura, and Bali (JAMALI) power system is critical to Indonesia's electrical infrastructure. In 2023, reliability issues were identified in the Krian-Gresik subsystem of East Java, particularly at the 500/150 kV Inter-Bus Transformer (IBT), which operated above 60% of its rated capacity, violating the N-1 contingency criterion. While IBT expansion was proposed to alleviate this loading, it introduced the risk of short-circuit currents exceeding circuit-breaker ratings. This study conducts the optimal bus coupler configuration to mitigate excessive short-circuit currents using a comparative analysis of Genetic Algorithm (GA) and Particle Swarm Optimization (PSO). The optimization incorporates operational constraints based on short-circuit current, bus voltage, and transformer loading indices to ensure system operational stability. Simulations conducted on a 44-bus model under different IBT expansion within the Krian-Gresik subsystem demonstrate that GA outperformed PSO, achieving the same optimal solution with a significantly higher success rate of 82.5% compared to 13.8% for PSO, and a 15.2% reduction in total computational time. The optimal configuration successfully reduces the IBT loading index from 42.36 to 34.36 and decreases the short-circuit current index from 187.81 to 120.54. The short-circuit currents at the TNDES, SWHAN, and RNKUT substations were reduced by up to 50%. Meanwhile, the voltage stability index increased from 77.93 to 104.70, indicating only minor voltage deviations within permissible limits. The overall system performance improved by 15.74%, establishing the Genetic Algorithm as a highly effective and efficient approach for enhancing security in the JAMALI power system.

**Keywords:** bus coupler, genetic algorithm (GA), Particle Swarm Optimization (PSO), loading performance index (LPI), short-circuit current index (SCI), voltage stability index (VSI).

## 1 Introduction

The demand for electrical energy in Indonesia continues to rise in line with economic growth, particularly in the East Java region. This region is projected to experience an


R. Adrian et al. (eds.), *Proceedings of the International Conference on Sustainable Energy: Toward Energy Transition and Net-Zero Emission (ICOSE 2025)*, Atlantis Highlights in Sustainable Development 4,
https://doi.org/10.2991/978-94-6463-944-5_6

average annual electricity demand growth of 4.12% that highlights the urgent need for a resilient and reliable transmission infrastructure to support the increasing load and ensure system stability [1]. Based on the 2023 System and Subsystem Vulnerability Report for the Java, Madura, and Bali grids, the 500/150kV IBT in the Krian-Gresik subsystem has experienced loading levels exceeding 60% when the subsystem loads are not properly distributed. To address this issue and in accordance with the 2021–2030 Electricity Supply Business Plan (RUPTL), PLN has formulated a strategic initiative to increase IBT capacity within this subsystem and to facilitate power evacuation from generation sources to ensure system reliability and effective load management. The electrical power system in East Java is divided into six main subsystems: Krian-Gresik 1,2; Krian 3,4,5; Ngimbang 1,2–Kediri 1,2; Kediri 3,4; Grati 1,2,3; and Paiton 1,2,3 [2]. Among these subsystems, the Krian-Gresik subsystem plays a critical role in supporting electricity transmission for industrial and metropolitan areas (see Fig. 1).

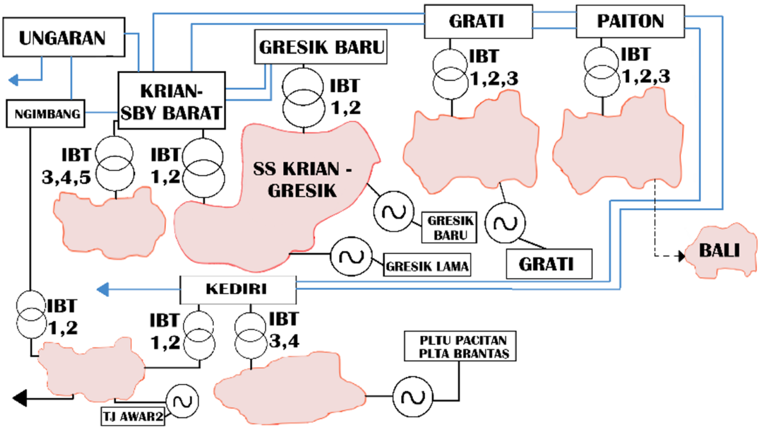


**Fig. 1.** Main subsystem of East Java Province

The addition of these transformers increases the complexity of the subsystem configuration during fault conditions in the transmission system. Parallel IBT connections between buses at different voltage levels reduce the system's equivalent impedance, which significantly raises short-circuit currents and may exceed the withstand capacity of protection equipment such as circuit-breaker. Excessive short-circuit current levels have become a critical concern in modern power systems, particularly in large-scale grids such as the China Power System and the Turkish Electricity Transmission System (TETS) [3].

The rise of fault current levels in modern power systems is primarily driven by the expansion of interconnection networks, the increasing integration of generation sources, and the growing concentration of electricity consumption. In response to these challenges, topology control has emerged as a key operational strategy which involves the strategic reconfiguration of the power grid to improve efficiency, reliability, and overall system security [4]. Among the various topology optimization techniques, busbar splitting is one of the most widely recognized approaches, as it modifies the network configuration to effectively limit the fault currents while ensuring operational parameters such as power flow and voltage stability remain within acceptable limits. In addition, this approach also offers economic advantages due to its relatively low implementation cost and short deployment timeline [5]. It has been successfully implemented in several real-world power systems, including the Oman Electricity Transmission System, the metropolitan network of the Electricity Generating Authority of Thailand, and the Istanbul Anatolian region of the Turkish Electricity Transmission Network [6]. However, reconfiguring the network is not a straightforward task, as increasing the number of split buses can weaken the overall stability and reliability of the power system.

Recent studies have employed conventional optimization methods, such as Mixed-Integer Linear Programming (MILP) and Mixed-Integer Nonlinear Programming (MINLP) to address power system configuration problems [7]. However, these classical approaches are often inadequate for large-scale, non-convex problems involving both linear and nonlinear components, as they are computationally expensive, exhibit slow convergence and become trapped in local optima due to premature convergence. Global metaheuristic algorithms such as Genetic Algorithms (GA), Particle Swarm Optimization (PSO), Differential Evolution (DE), Simulated Annealing (SA), Tabu Search (TS), and Evolutionary Programming (EP) offer greater flexibility in solving nonlinear and multi-objective optimization problems that are often difficult to handle using conventional methods. Among these, GA and Particle Swarm Optimization (PSO) have emerged as particularly prominent due to their conceptual simplicity, straightforward implementation, and established historical track record [8].

In previous studies focused on bus layout optimization, GA demonstrated slightly better performance and a faster convergence rate than Binary Particle Optimization (BPSO), successfully reducing the short-circuit performance index to zero. However, GA generally requires more computational time compared to PSO [9,10]. These findings establish GA's strong potential for security-constrained power system optimization.

Although GA and PSO have been applied in previous studies, its application to bus coupler optimization under Inter-Bus Transformer (IBT) expansion conditions has not been thoroughly explored. This research gap underscores the need for further investigation into how optimization can be effectively employed to determine optimal bus coupler configurations that maintain operational reliability and system security. This study aims to identify the optimal bus coupler configuration during IBT expansion to mitigate three-phase short-circuit currents while ensuring that bus voltages and IBT loading remain within permissible operating limits. A comparative performance analysis is also evaluated to validate the computational efficiency and solution quality of GA against PSO.

# 2 Problem Formulation

## 2.1 Overview of the East Java 500 kV Grid

The 500 kV transmission network in East Java is supported by six major substations (GITET): Krian, Gresik, Grati, Kediri, Paiton, and Ngimbang. These substations form an interconnected system with a combined installed capacity of approximately 9,000 MVA. The power system in East Java Province is divided into seven subsystems, among which the Krian-Gresik subsystem plays a crucial role in supplying electricity to Surabaya City, Gresik Regency, Tuban Regency, Lamongan Regency, and the Madura region.

Due to the growing electricity demand from critical industrial zones, an additional 500/150 kV IBT with a capacity of 1 × 500 MVA was installed at the GITET Krian substation. Moreover, in line with the targets of the 2021–2030 RUPTL, two additional 500/150 kV IBTs, each rated at 500 MVA, are scheduled to be reconfigured at the GITET Waru substation. These transformers will feed the downstream 150 kV substations. The integration of these IBTs into the Krian-Gresik subsystem requires a comprehensive evaluation to ensure that their operation preserves the security and stability of the overall power system.

## 2.2 Short-Circuit Current Index

The short-circuit capacity at a bus is a critical parameter used for accurately sizing busbars and determining the appropriate interrupting capacity of circuit-breaker [11]. The magnitude of this short-circuit current depends on the equivalent impedance seen from the faulted bus which is often represented by using Thevenin's equivalent impedance model. Typically, a three-phase fault produces the highest short-circuit current compared to other fault types [12]. Under balanced three-phase fault conditions, the fault current at a specific bus $k$ can be expressed in Eq. (1) as follows:

$$I_{sc,k} = \frac{V_{th,k}(0)}{Z_{th,k}+Z_f} \tag{1}$$

where $I_{sc,k}$ is the three-phase short-circuit current at bus $k$, $V_{th,k}(0)$ is the pre-fault voltage or Thevenin voltage at bus $k$, $Z_{th,k}$ is Thevenin equivalent impedance at bus $k$, and $Z_f$ is the fault impedance.

The Eq. (1) shows that an increase in total impedance will decrease the level of short-circuit current. Thus, incorporating the short-circuit current into a performance index is essential for effectively assessing and comparing the severity of disturbances at various locations within the power system [13]. To facilitate this evaluation, a short-circuit performance index is formulated in Eq. (2) to determine whether the fault current at each bus exceeds its maximum allowable limit [9].

$$PI_{sc} = \begin{cases} \left(\frac{I_{sc,k}}{W_i}\right)^{2n}, if\ I_{sc,k} > SCC_k^{limit} \\ 0,\ otherwise \end{cases} \tag{2}$$

where $PI_{sc}$ is the short-circuit current performance index, $I_{sc,k}$ is the normalized fault current, $SCC_k^{limit}$ is the short-circuit current limit, $W_i$ is the scaling factor to normalize the index, and $n$ is the penalty exponent.

## 2.3 Voltage Stability Index

Voltage stability refers to the ability of a power system to maintain acceptable voltage levels under normal operating conditions and following a disturbance. This problem commonly arises in power systems with insufficient reactive power support, particularly under heavy loading conditions [14]. As part of voltage stability assessment, a voltage performance index $PI_V$ is employed to quantify the severity of voltage deviations across all buses. This index measures the deviation between the actual and rated bus voltages while incorporating appropriate weighting factors, as expressed in Eq. (3).

$$PI_V = \sum_{k=1}^{n} \frac{W_n}{2n} \left( \frac{|V_k| - \left|V_k^{rated}\right|}{\Delta V_k^{lim}} \right) \quad (3)$$

where $PI_V$ is the voltage performance index, $W_v$ is the weighting coefficient for bus $k$, $|V_k|$ is the voltage magnitude at bus $k$, $\left|V_k^{rated}\right|$ is the rated voltage at bus k, $\Delta V_k^{lim}$ is permissible voltage deviation (0.95-1.05 p.u), and $n$ is the penalty exponent.

## 2.4 Transformer Loading Performance Index

To evaluate the risk of overloads, a performance index is employed as a quantitative measure of transformer loading relative to their maximum allowable ratings as shown in Eq. (4) [15].

$$PI_p = \sum_{k=1}^{n} \frac{W_v}{2n} \left( \frac{P_l}{P_l^{max}} \right) \quad (4)$$

where $PI_p$ is the transformer loading performance index, $P_l$ $is$ the power transferred through the IBT, $P_l^{max}$ is the rated capacity of the IBT, $W_v$ is the weighting coefficient for the index, and $n$ is the penalty exponent.

## 2.5 Optimization Method

**Genetic Algorithm (GA).** The Genetic Algorithm (GA) has demonstrated robust performance in solving large-scale and complex optimization problems by emulating the principles of natural evolution. It is a widely used evolutionary optimization method that employs biologically inspired operators, such as selection, crossover, and mutation, to perform global searches over complex, high dimensional solution spaces [16]. The effectiveness is primarily influenced by three key parameters: population size, crossover rate, and mutation rate, which control the balance between exploration and exploitation in the solution space. GA operates on the evolutionary principle that high-fitness individuals are more likely to survive and propagate, while inferior solutions are gradually eliminated over successive generations, ultimately converging toward optimal or near optimal solutions [17]. In this study, GA is adapted to solve the optimal bus coupler configuration problem, as illustrated in Fig. 2 [18].

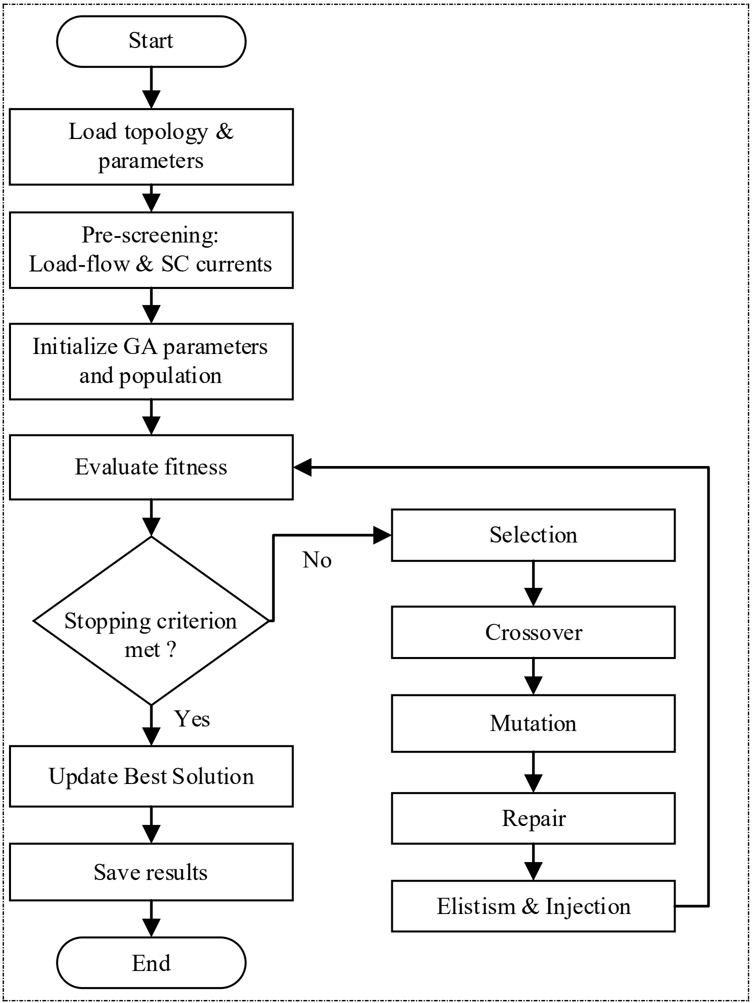


**Fig. 2.** Flowchart of the GA for optimal bus coupler configuration

The optimization process starts with initializing DIgSILENT study cases and running AC power flow to set the operating point. Critical buses are identified from three-phase short-circuit results, and their bus-coupler switching states form the GA chromosome. A population evolves through selection, crossover, mutation, and elitism, with fitness evaluated from a weighted sum of performance indices (short-circuit current, bus voltage, and IBT loading) while penalties are applied for constraint violations. The algorithm terminates when the maximum number of generations is reached or when no significant improvement in fitness is observed.

**Particle Swarm Optimization (PSO).** Particle Swarm Optimization (PSO) is a powerful metaheuristic algorithm modeled on the collective intelligence observed in nature, such as the synchronized movement of bird flocks. PSO algorithm distinguishes itself from other population-based metaheuristics, such as genetic algorithms that rely on biologically inspired operators like crossover and mutation. Instead, PSO optimizes a problem by having a population of candidate solutions, known as particles, navigating the search space through a process of directed velocity and position updates [19].

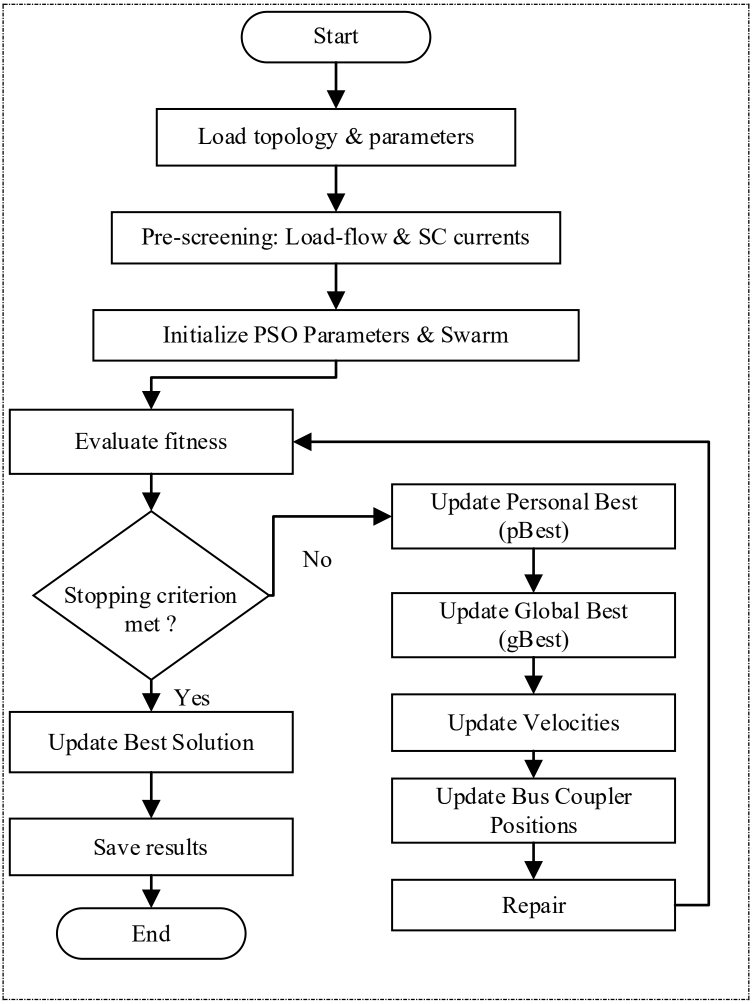


**Fig. 3.** Flowchart of the PSO for optimal bus coupler configuration

In this study, PSO is adapted to solve the optimal busbar configuration problem as illustrated in Fig. 3. Each particle's position represents a potential solution for bus coupler configuration, while its velocity dictates both the direction and magnitude of its movement. The process begins with a swarm of particles initialized at random positions. The core intelligence of PSO emerges from the iteration, where each particle calculates its new velocity by balancing three forces: its own inertia ($w$), the attraction to the best location it has personally discovered ($p_{best}$), and the attraction to the best location found by any particle in the entire swarm ($g_{best}$). This mechanism allows the swarm to efficiently explore the search space, balancing individual memory with social learning, and progressively converges the particles toward the most promising regions to locate the optimal solution.

# 3 Methodology

## 3.1 Network Configuration: Krian-Gresik Subsystem

The network configuration is evaluated based on IBT expansion as follows:

- Case 1: Base configuration.
- Case 2: IBT-6 is installed at the GITET Krian substation. It operates in parallel with IBT-1 and IBT-2.
- Case 3: The system in Case 2 is added with two IBTs (IBT-1 and IBT-2) at GITET Waru substation.

In this study, the Krian-Gresik subsystem is adopted as the test network as illustrated in

The modified network model represents the system configuration.

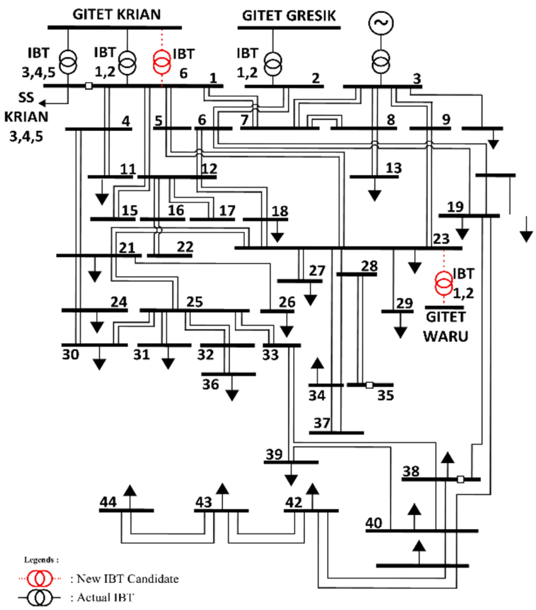


**Fig. 4.** Modified Krian-Gresik subsystem

The total peak load in this subsystem is 1,830 MW, while the available net supply capacity reaches 2,320 MW. The 500/150 kV IBTs at GITET Krian and GITET Gresik facilitate power transfer to the downstream 150 kV substations. The GITET Gresik substation is equipped with two IBTs, each rated at 500 MVA. Meanwhile, the GITET Krian substation is equipped with five IBTs, of which IBT-1 and IBT-2 rated at 500 MVA, operate in parallel with IBT-1 and IBT-2 of Gresik to form a subsystem. The Krian-Gresik subsystem is modeled as a network comprising generator buses and load buses. The generator buses include the Gresik Lama substation and the Gresik Baru substation. The load buses are represented by a total of 44 buses as shown in Table 1.

**Table 1.** Normal Bus Configurations in the Krian-Gresik Subsystem.

| Bus | Substation | Coupler Status | Bus | Substation | Coupler Status |
|---|---|---|---|---|---|
| 1 | SBBRAT | Closed | 23 | WARU | Closed |
| 2 | GRESIK | Closed | 24 | SBSEL | Closed |
| 3 | GRLMA | Closed | 25 | SLILO | Closed |
| 4 | KLANG | Closed | 26 | HJAYA | Closed |
| 5 | DARMO | Closed | 27 | ISPDO | Closed |
| 6 | TNDES | Closed | 28 | BDRAN | Closed |
| 7 | ALTAP | Closed | 29 | JSTEL | Closed |
| 8 | SGMD-B | Closed | 30 | KSARI | Closed |
| 9 | SKREP | Closed | 31 | WKRMO | Closed |
| 10 | WLMAR | Closed | 32 | NGGEL | Closed |
| 11 | BAMBE | Closed | 33 | KJRAN | Closed |
| 12 | SWHAN | Closed | 34 | NBRAN | Closed |
| 13 | PKMIA | Closed | 35 | SDRJO | Open |
| 14 | PERAK | Closed | 36 | SIMPG | Closed |
| 15 | KPANG | Closed | 37 | SDATI | Closed |
| 16 | UDAAN | Closed | 38 | KDING | Open |
| 17 | KRBAN | Closed | 39 | GLMUR | Closed |
| 18 | GNSARI | Closed | 40 | BKLAN | Closed |
| 19 | UJUNG | Closed | 41 | SAMPG | Closed |
| 20 | PTISM | Closed | 42 | PKSAN | Closed |
| 21 | RNKUT | Closed | 43 | GULUK | Closed |
| 22 | GBONG | Closed | 44 | SMNEP | Closed |

### 3.2 Problem Formulation

**Objective Function.** The objective is to minimize a weighted sum of normalized performance indices: short-circuit, voltage stability, and transformer loading. The performance index is combined into a single objective and expressed in per unit (p.u) on the system base. The optimal bus coupler configuration is obtained by minimizing the total performance indices as shown in equation (5)-(6) [20].

$$min_x \, f(x) = PI_{tot}(x) \tag{5}$$

$$PI_{tot}(x) = W_{sc}.PI_{sc}(x) + W_V.PI_V(x) + W_P.PI_P(x) \tag{6}$$

**Constraints.** The optimization problem is subject to the following operational constraints:

- The real and reactive power of generator limit:

$$P_{G,k}^{min} \leq |P_{G,k}| \leq P_{G,k}^{max} \; , \; Q_{G,k}^{min} \leq |Q_{G,k}| \leq Q_{G,k}^{max} \tag{7}$$

- Bus voltage limit:

$$V_k^{min} \leq |V_k| \leq V_k^{max} \tag{8}$$

- Bus coupler split constraint:

$$\sum_{i=1}^{n}(1 - e_i) = 2, \; e_i \in \{0.1\} \tag{9}$$

where $n$ is the total number of bus couplers. The binary variable $e_i$ denotes the status of the $i$th bus coupler: $e_i$= 0 if the coupler is open (buses split) and $e_i$= 1 if it is closed (buses connected).

**Parameter.** To ensure a balance between convergence speed and population diversity while avoiding premature convergence, the GA and PSO parameters are selected as summarized in Table 2.

**Table 2.** Optimization Algorithm Parameters

| Parameters | GA | PSO |
|---|---|---|
| Population/Swarm Size | 20 | 20 |
| Maximum Iterations | 15 | 15 |
| Crossover probability | 0.8 | - |
| Mutation probability | 0.05 | - |
| Inertia weight ($w$) | - | 0.7 |
| Coefficient (c1, c2) | | 1.5 , 1.5 |
| Selection Method | Tournament | - |
| Elitism | 1 | - |

The parameters are selected to achieve a balance between convergence speed and population diversity. Convergence speed ensures that the algorithm can approach the best fitness value within a reasonable computational time, which is critical when solving large-scale power system problems.

## 4 Results and Discussion

This section presents the optimization results for the Krian-Gresik subsystem under IBT expansion.

### 4.1 Optimization Results of Bus Coupler Configuration

The impact of IBT expansion on bus short-circuit levels in the Krian–Gresik subsystem is illustrated in Fig. 5. In Cases 1 and 2, all buses operate within the permissible three-phase short-circuit limits which indicate that no further bus splitting is required. In contrast, Case 3 exhibits seven substations with short-circuit levels exceeding the 40 kA circuit-breaker rating. To mitigate this issue, optimization is applied with the objective of reducing fault currents while maintaining acceptable operational constraints.

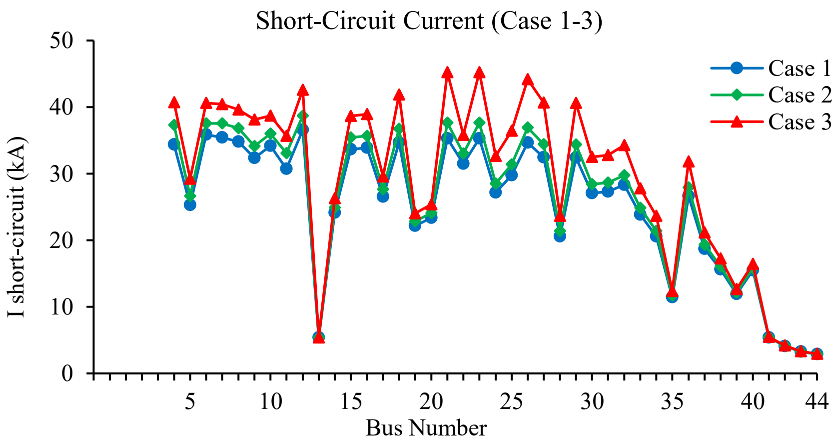


**Fig. 5.** Short-circuit current profiles at buses for Cases 1–3.

The graphical results demonstrate that in both Case 1 and Case 2, the short-circuit currents remain within permissible limits, thus requiring no optimization and resulting in all bus couplers maintaining their closed status. In contrast, Case 3 requires optimization due to excessive short-circuit currents, for which both Genetic Algorithm (GA) and Particle Swarm Optimization (PSO) methods are employed.

The optimization results, summarized in

Table **3**, show that opening the bus couplers at the Rungkut (RNKUT) and Sawahan (SWHAN) substations effectively mitigates the short-circuit issues while ensuring secure system operation across all seven substations.

**Table 3.** IBT configuration and bus coupler status

| Description | Case 1 | Case 2 | Case 3 |
|---|---|---|---|
| IBT configuration | | | |
| GITET KRIAN | IBT-1, IBT-2 | IBT-1, IBT-2, IBT-6 | IBT-1, IBT-2, IBT-6 |
| GITET WARU | None | None | IBT-1, IBT-2 |
| Bus coupler status | | | |
| ALTAP | Closed | Closed | Closed |
| GNSRI | Closed | Closed | Closed |
| KLANG | Closed | Closed | Closed |
| RNKUT | Closed | Closed | Open |
| SWHAN | Closed | Closed | Open |
| TNDES | Closed | Closed | Closed |
| WARU | Closed | Closed | Closed |

The optimization results for Case 3 are illustrated in Fig. 6 which shows a substantial reduction in short-circuit currents at several critical substations.

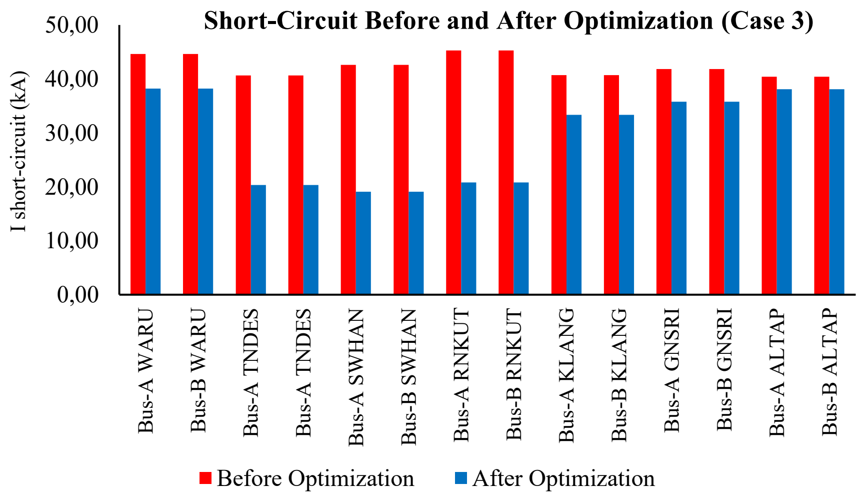


**Fig. 6.** Short-circuit currents in Case 3.

The graph shows that the current at WARU substation decreased from 44.61 kA to 38.21 kA, representing a 14.3% reduction at both Bus-A and Bus-B. More significant improvements are observed at TNDES substation, where the current decreased from 40.63 kA to 20.36 kA with a 49.9% reduction, and at Bus-A and Bus-B SWHAN, where the current decreased from 42.58 kA to 19.09 kA with a 55.2% reduction. Similarly, Bus-A and Bus-B RNKUT shows a decrease from 45.25 kA to 20.82 kA, representing a 54% reduction, while Bus-A and Bus-B KLANG decreased from 40.70 kA to 33.35 kA, representing an 18.1% reduction. Additional reductions were also observed at Bus-A and Bus-B GNSRI (14.5%), and Bus-A and Bus-B ALTAP (5.8%).

In addition to the reduction in short-circuit currents, the voltage profile of each bus is evaluated for each scenario, as shown in Fig. 7. The graph indicates that the voltage at each bus remains within the permissible operating limits of 0.95 to 1.05 p.u. However, following the bus coupler splitting optimization, a decrease in voltage is observed at certain buses.

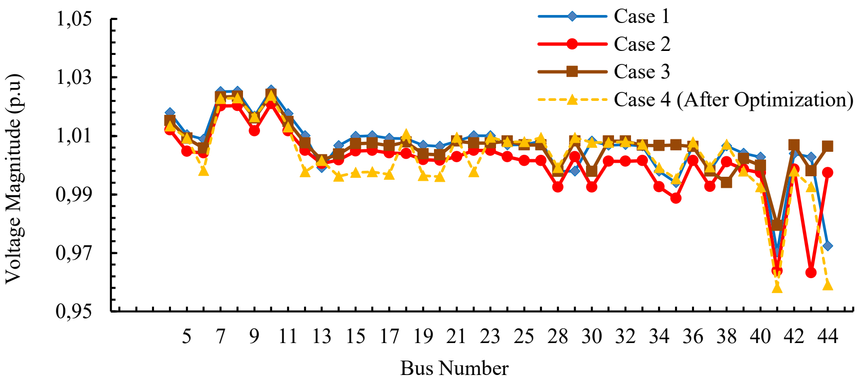


**Fig. 7.** Voltage profiles of buses

As summarized in Table 4, a comparative analysis of the total performance indices illustrates the effect of the bus coupler configuration on the system's operational constraints.

**Table 4.** Performance indices before and after optimization

| Case | $PI_{sc}$ | | $PI_V$ | | $PI_p$ | | $PI_{tot}$ | |
|---|---|---|---|---|---|---|---|---|
| | Before | After | Before | After | Before | After | Before | After |
| Case 1 | 135.71 | - | 77.61 | - | 67.39 | - | 280.71 | - |
| Case 2 | 150.75 | - | 73.82 | - | 49.19 | - | 273.76 | - |
| Case 3 | 187.81 | 120.54 | 77.93 | 104.70 | 42.36 | 34.36 | 308.10 | 259.60 |

In Case 1, the performance indices indicate that the system experiences moderate levels of short-circuit currents and IBT loading, with no violations in bus voltage. In Case 2, the addition of a 500 MVA IBT-6 at Krian Substation, operating in parallel with IBT-1 and IBT-2, significantly increased the bus short-circuit levels. The short-circuit index ($PI_{sc}$) rises from 135.71 to 150.75, while the IBT loading index ($PI_p$) decreases from 280.71 to 273.76 as the subsystem loading is more evenly distributed. Additionally, the voltage stability index ($PI_V$) decreases from 77.61 to 73.82, that indicates improved voltage levels at certain buses.

In contrast, Case 3 involves the addition of two IBTs (IBT-1 and IBT-2) at Waru Substation, where the GA identifies short-circuit violations. This results in higher total performance indices due to the increased fault current. The voltage performance index shows an increase in voltage deviation. Meanwhile, the IBT loading index decreases from 49.19 to 42.36. For Case 4, after the bus coupler splitting optimization, the total performance indices decreased by approximately 15.74%, from 308.10 to 259.60 due to the reduction in the short-circuit level within the subsystem. This reduction in performance signifies a more balanced and stable system operation, characterized by lower short-circuit currents and improved load distribution among the Inter-Bus Transformers (IBTs). However, the bus voltage index shows a notable increase from 77.93 to 104.70, suggesting that minor voltage deviations occurred at certain buses following the bus splitting optimization.

### 4.2 Comparative Analysis of Optimization Algorithms

A comparative performance evaluation between a Genetic Algorithm (GA) and Particle Swarm Optimization (PSO) was conducted for the bus coupler configuration problem in the Krian-Gresik subsystem (Case 3). The algorithms were implemented in Python, integrated with DIgSILENT Power Factory via its API, and executed on a standard PC (Intel Core i7, 16 GB RAM) under identical conditions to ensure a fair comparison. The comparative analysis, summarized in Table 5, shows a significant difference in algorithmic performance and computational efficiency.

**Table 5.** Performance Comparison of GA and PSO Algorithms

| Performance Metric | GA | PSO |
|---|---|---|
| Success Rate | 82.5% | 13.8% |
| Average Time per Evaluation | 13.425 s | 15.836 s |
| Optimal Configuration | 1110011 | 1110011 |
| Total Computational Time | 1073.99 s | 1266.90 s |

The results show that GA demonstrated better performance than PSO, achieving a significantly higher success rate (82.5% vs. 13.8%) and a 15.2% faster computational time. Despite both methods finding the same optimal configuration, GA's enhanced reliability and efficiency established it as the more suitable approach for determining the optimal configuration of a subsystem network subject to operational constraints.

## 5 Conclusion

This study successfully demonstrates the optimal bus coupler configuration of a subsystem in network configuration mitigates excessive short-circuit currents resulting from the expansion of IBTs by strategically selecting and splitting the targeted bus couplers. The proposed optimization approach strategically determined the optimal status of bus couplers, specifically opening the RNKUT and SWHAN couplers, to limit fault currents while maintaining operational constraints.

The comparative analysis confirmed GA as more reliable and efficient than PSO, securing the optimal solution with a success rate of 82.5% in finding the optimal solution and completing the optimization 15.2% faster. The results confirm the method's high efficacy: the short-circuit current index was reduced from 187.81 to 120.54, and the IBT loading index was improved from 42.36 to 34.36. Although optimization improved the overall system performance by 15.74%, it adversely affected the voltage stability index, which increased from 77.93 to 104.70, indicating a reduction in stability margins. This finding highlights a fundamental trade-off in power system design, where configurations optimized to limit short-circuit currents may compromise voltage stability during contingencies or periods of elevated demand. Ensuring system reliability therefore requires a balanced approach that integrates fault protection and voltage stability considerations. Future work should extend network optimization studies to account for contingencies involving inter-bus transformers (IBTs) and transmission lines to achieve more comprehensive system resilience.

**Acknowledgments.** This research was financially and technically supported by Universitas Gadjah Mada and PLN Company.

**Disclosure of Interests.** The authors have no competing interests to declare that are relevant to the content of this article.

## References

1. PT PLN (Persero): Rencana Usaha Penyediaan Tenaga Listrik (RUPTL) 2021–2030. PT PLN (Persero), Jakarta, Indonesia (2021)
2. PT PLN (Persero): Evaluasi Operasi Sistem Jawa Madura Bali Tahun 2024. Unit Induk Pusat Pengatur Beban, Jakarta Selatan (2024)
3. Dogan, E., Yorukeren, N.: Enhancement of transmission system security with Archimedes optimization algorithm. *Turkish J. Electr. Power Energy Syst.* **2**(2), 115–123 (2022)
4. Deepika, N.M., Shrivastava, A., Rajalakshmi, B., Nijhawan, G., Yadav, D.K., Issa, A.A.: Advanced topology control schemes for power flow management in complex transmission networks with high renewable penetration. In: *Proc. Int. Conf. Trends Quantum Comput. Emerging Business Technol. (TQCEBT)*, Pune, India, pp. 1–6 (2024)
5. Kanlaya, P., Hoonchareon, N.: Combined bus splitting and line bypassing for short-circuit currents limitation. In: *Proc. 10th Int. Conf. Electr. Eng./Electronics, Comput., Telecommun. Inf. Technol. (ECTICON)*, Krabi, Thailand, pp. 1–6 (2013)
6. Wang, L., Chiang, H.-D.: Busbar splitting for enhancing voltage stability under contingencies. *Sustain. Energy Grids Netw.* **34**, 101010 (2023)
7. Gharibpour, H., Aminifar, F., Haji Bashi, M.: Short-circuit-constrained transmission expansion planning with bus splitting flexibility. *IET Gener. Transm. Distrib.* **12**(1), 217–226 (2018)
8. Nassef, A.M., Abdelkareem, M.A., Maghrabie, H.M., Baroutaji, A.: Review of metaheuristic optimization algorithms for power systems problems. Sustainability 15(12), 9434 (2023). https://doi.org/10.3390/su15129434

9. Dogan, E., Yorukeren, N.: Optimal bus layout in transmission system by using meta-heuristic approaches. *Electr. Power Components Syst.* **48**(12–13), 1390–1400 (2020)
10. Watthanasarn, N.R., Yeap, Y.M., Ngamroo, T., Hongesombut, K., Ng, H.K.: Optimal bus splitting for short-circuit current limitation in metropolitan area. *IET Gener. Transm. Distrib.* **12**(19), 4285–4294 (2018)
11. Saadat, H.: Power System Analysis. McGraw-Hill, New York (1999)
12. Abdulkareem, A., Awosope, C.O.A., Awelewa, A.A.: The use of three-phase fault analysis for rating circuit-breaker on Nigeria 330 kV transmission lines. *J. Eng. Appl. Sci.* **11**(12), 2612–2622 (2016)
13. Putri, M.D.M., Afandi, A.N.: Performance index analysis (PIA) for N-1 contingency transmission in 150 kV electricity system. In: *Proc. Int. Conf. Electr., Electron. Inf. Eng. (ICEEIE)*, Denpasar, Indonesia, pp. 1–5 (2019)
14. Kundur, P.: Power System Stability and Control. McGraw-Hill, New York (1994)
15. Fauziah, D., Mulyadi, Y.: Contingency analysis of South Bandung electric power system. *IOP Conf. Ser.: Mater. Sci. Eng.* **180**, 012053 (2017)
16. Heidari, A.A., Mirjalili, S., Faris, H., Aljarah, I., Mafarja, M., Chen, H.: A review on genetic algorithm: Past, present, and future. *Mach. Learn. Appl.* **3**, 100204 (2021)
17. Singh, S.N., Srivastava, S.C.: Formulation of loss minimization problem using genetic algorithm and particle swarm optimization technique. In: *Proc. Int. Conf. Intell. Syst. Appl. Power Syst.*, Kaohsiung, Taiwan, pp. 1–6 (2007)
18. Rao, K.V.S., Kalavathi, K.: A review on applications of heuristic optimization algorithms in modern power system. *Int. J. Electr. Power Energy Syst.* **82**, 494–507 (2016)
19. Wen, C., Wang, L., Ren, X.: General particle swarm optimization algorithm. In: Proc. 2023 IEEE 2nd International Conference on Electrical Engineering, Big Data and Algorithms (EEBDA), pp. 1–6 (2023)
20. Cheng, P., Sulaiman, J., Ghazali, K., Ali, M.K.M., Xu, M.M.: Newton iteration with weighted exponential penalty function for solving multi-objective constrained optimization problems. *J. Qual. Meas. Anal.* **21**(2), 93–108 (2025)